

---

# Overlapping Spaces for Compact Graph Representations

---

**Kirill Shevkunov**

Yandex, MIPT  
Moscow, Russia  
shevkunov.ks@phystech.edu

**Liudmila Prokhorenkova**

Yandex, MIPT, HSE University  
Moscow, Russia  
ostroumova-la@yandex.ru

## Abstract

Various non-trivial spaces are becoming popular for embedding structured data such as graphs, texts, or images. Following spherical and hyperbolic spaces, more general *product spaces* have been proposed. However, searching for the best configuration of product space is a resource-intensive procedure, which reduces the practical applicability of the idea. We generalize the concept of product space and introduce an *overlapping space* that does not have the configuration search problem. The main idea is to allow subsets of coordinates to be shared between spaces of different types (Euclidean, hyperbolic, spherical). As a result, parameter optimization automatically learns the optimal configuration. Additionally, overlapping spaces allow for more compact representations since their geometry is more complex. Our experiments confirm that overlapping spaces outperform the competitors in graph embedding tasks. Here, we consider both *distortion* setup, where the aim is to preserve distances, and *ranking* setup, where the relative order should be preserved. The proposed method effectively solves the problem and outperforms the competitors in both settings. We also perform an empirical analysis in a realistic information retrieval task, where we compare all spaces by incorporating them into DSSM. In this case, the proposed overlapping space consistently achieves nearly optimal results without any configuration tuning. This allows for reducing training time, which can be significant in large-scale applications.

## 1 Introduction

Building vector representations of various objects is one of the central tasks of machine learning. Word embeddings such as Glove [21] and Word2Vec [18] are widely used in natural language processing; a similar Prod2Vec [7] approach is used in recommendation systems. There are many algorithms proposed for graph embeddings, e.g., Node2Vec [8] and DeepWalk [22]. Recommendation systems often construct embeddings of a bipartite graph that describes interactions between users and items. Such embeddings can be constructed via matrix factorization techniques such as ALS [10].

For a long time, embeddings were considered exclusively in  $\mathbb{R}^n$ . However, the hyperbolic space was shown to be more suitable for graph, word, and image representations due to the underlying hierarchical structure [12, 19, 20, 25]. Going beyond spaces of constant curvature, a recent study [9] proposed *product spaces*, which combine several copies of Euclidean, spherical, and hyperbolic spaces. While these spaces demonstrate promising results, the optimal signature (types of combined spaces and their dimensions) has to be chosen via brute force, which may not be acceptable in large-scale applications.

In this paper, we propose a more general metric space called *overlapping space* together with an optimization algorithm that trains signature *simultaneously* with embedding allowing us to avoid

brute-forcing. The main idea is to allow coordinates to be shared between different spaces, which allows us to significantly reduce the number of coordinates needed.

Importantly, we also suggest adding non-metric approaches such as *weighted inner product* [13] as an additional similarity measure complementing metric ones, whereas usually metric methods are compared with metric methods, which, as we show below, can be suboptimal. Moreover, we offer a flexible hybrid measure *OS-Mixed* that allows us to take the best of the two approaches and can be extended with additional base metric spaces and non-metric measures.

To validate the usefulness of the proposed overlapping space, we provide an extensive empirical evaluation for the task of graph embedding, where we consider both distortion-based and ranking-based objectives. In both cases, the proposed measure outperforms the competitors. We also compare the spaces in information retrieval and recommendation tasks, for which we apply them to train embeddings via DSSM [11]. Our method works comparable to the best signature tested in these cases, while it does not require brute-forcing for the best signature. Thus, using the overlapping space may significantly reduce the training time, which can be crucial in large-scale applications.

## 2 Background and related work

### 2.1 Embeddings and loss functions

For a graph  $G = (V, E)$  an embedding is a mapping  $f : V \rightarrow U$ , where  $U$  is a metric space equipped with a distance  $d_U : U \times U \rightarrow \mathbb{R}_+$ .<sup>1</sup> On the graph, one can consider a shortest path distance  $d_G : V \times V \rightarrow \mathbb{R}_+$ . In the graph reconstruction task, it is expected that a good embedding preserves the original graph distances:  $d_G(v, u) \approx d_U(f(v), f(u))$ . The most commonly used evaluation metric is *distortion*, which averages relative errors of distance reconstruction over all pairs of nodes:

$$D_{avg} = \frac{2}{|V|(|V| - 1)} \sum_{(v, u) \in V^2, v \neq u} \frac{|d_U(f(v), f(u)) - d_G(v, u)|}{d_G(v, u)}. \quad (1)$$

While commonly used in graph reconstruction, distortion is not the best choice for many practical applications. For example, in recommendation tasks, one usually deals with a partially observed graph (some positive and negative element pairs), so a huge graph distance between nodes in the observed part does not necessarily mean that the nodes are not connected by a short path in the full graph. Also, often only the order of the nearest elements is essential while predicting distances to faraway objects is not critical. In such cases, it is more reasonable to consider a local ranking metric, e.g. the mean average precision (mAP) that measures the relative closeness of the relevant (adjacent) nodes compared to the others:<sup>2</sup>

$$\text{mAP} = \frac{1}{|V|} \sum_{v \in V} \text{AP}(v) = \frac{1}{V} \sum_{v \in V} \frac{1}{\deg(v)} \sum_{u \in N_v} \frac{|N_v \cap R_v(u)|}{|R_v(u)|}, \quad (2)$$

$$R_v(u) = \{w \in V | d_U(f(v), f(w)) \leq d_U(f(v), f(u))\}, N_v = \{w \in V | (v, w) \in E\}.$$

Note that mAP cannot be directly optimized since it is not differentiable. In our experiments, we use the following probabilistic loss function as a proxy:<sup>3</sup>

$$L_{proxy} = - \sum_{(v, u) \in E} \log P((v, u) \in E) = - \sum_{(v, u) \in E} \log \frac{\exp(-d_U(f(v), f(u)))}{\sum_{w \in V} \exp(-d_U(f(v), f(w)))}. \quad (3)$$

Note that when substituting  $d_U(x, y) = c - f(x)^T f(y)$  (assuming that  $f(x) \in \mathbb{R}^n$ , so the dot product is defined), we get the standard word2vec loss function.

### 2.2 Spaces, distances, and similarities

In the previous section, we assumed that  $d_U : U \times U \rightarrow \mathbb{R}_+$  is an arbitrary distance. In this section, we discuss particular choices often assumed in the literature.

<sup>1</sup>Note that any discrete metric space corresponds to a weighted graph, so graph terminology is not restrictive.

<sup>2</sup>For mAP, the relevance labels are assumed to be binary (unweighted graphs). If a graph is weighted, then we say that  $N_v$  consists of the closest element to  $v$  (or several closest elements if the distances to them are equal).

<sup>3</sup>See Table 5 of the supplemental material with other ways of converting distance to probability.

For many years, Euclidean space was the primary choice for structured data embeddings [6]. For two points  $x, y \in \mathbb{R}^d$ , Euclidean distance is defined as  $d_E(x, y) = \left( \sum_{i=1}^d (x_i - y_i)^2 \right)^{1/2}$ .

Spherical spaces were also found to be suitable for some applications [17, 23, 29]. Indeed, in practice, vector representations are often normalized, so cosine similarity between vectors is a natural way to measure their similarity. This naturally corresponds to a spherical space  $S_d = \{x \in \mathbb{R}^{d+1} : \|x\|_2^2 = 1\}$  equipped with a distance  $d_S(x, y) = \arccos(\langle x, y \rangle)$ .

In recent years, hyperbolic spaces also started to gain popularity. Hyperbolic embeddings have shown their superiority over Euclidean ones in a number of tasks, such as graph reconstruction and word embedding [19, 20, 24, 25]. To represent the points, early approaches used the Poincare model of the hyperbolic space [19], but later it has been shown that the hyperboloid (Lorentz) model may lead to more stable results [20]. In this work, we also adopt the hyperboloid model  $H_d = \{x \in \mathbb{R}^{d+1} | \langle x, x \rangle_h = 1, x_1 > 0\}$  equipped with a distance  $d_H = \operatorname{arccosh}(\langle x, y \rangle_h)$ , where  $\langle x, y \rangle_h := x_1 y_1 - \sum_{i=2}^{d+1} x_i y_i$ .

Going even further, a recent paper [9] proposed more complex *product spaces* that combine several copies of Euclidean, spherical, and hyperbolic spaces. Namely, the overall dimension  $d$  is split into  $k$  parts (smaller dimensions):  $d = \sum_{i=1}^k d_i$ ,  $d_i > 0$ . Each part is associated with the space  $D_i \in \{E_{d_i}, S_{d_i}, H_{d_i}\}$  and scale coefficient  $w_i \in \mathbb{R}_+$ . Varying scale coefficients corresponds to changing curvature of hyperbolic and spherical spaces, while in Euclidean space this coefficient is not used ( $w_i = 1$ ). Then, the distance in the product space is defined as:

$$d_P(x, y) = \sqrt{\sum_{i=1}^k w_i d_{D_i}(x[t_{i-1} + 1 : t_i], y[t_{i-1} + 1 : t_i])^2},$$

where  $t_0 = 0$ ,  $t_i = t_{i-1} + d_i$ , and  $x[s : e]$  is a subvector  $(x_s, \dots, x_e) \in \mathbb{R}^{e-s+1}$ . If  $k = 1$ , we get a standard Euclidean, spherical, or hyperbolic space. In [9], it is proposed to learn an embedding and scale coefficients  $w_i$  simultaneously. However, choosing the optimal signature (how to split  $d$  into  $d_i$  and which types of spaces to choose) is challenging. A heuristics proposed in [9] allows to guess types of spaces if  $d_i$ 's are given. If  $d_1 = d_2 = 5$ , this heuristics agrees well with the experiments on three considered datasets. The generalizability of this idea to other datasets and configurations is unclear. In addition, it cannot be applied if a dataset is partially observed (e.g., there are several known positive-negative pairs), i.e., graph distances cannot be computed. Hence, in practice, it is more reliable to choose a signature via the brute-force, which can be inapplicable on large datasets.

Another way to measure objects' similarity, which is rarely compared with metric methods but is frequently used in practical applications, is via the dot product of vectors  $x^T y$  or its weighted version  $x^T W y$  with a diagonal matrix  $W$ , which is also known as a weighted inner product [13]. Such measures cannot be converted to a distance via a monotone transformation; however, they can be used to predict similarity or dissimilarity between objects, which is often sufficient in practice, especially when ranking metrics are used.

In this paper, we stress that when comparing different methods, both metric and non-metric variants should be used when appropriate because different methods are better for different tasks. In particular, dot-product allows one to easily differentiate between more popular and less popular items (the vector norm can be considered a measure of popularity). This feature is also attributed to hyperbolic spaces, where more popular items are located closer to the origin.

### 2.3 Optimization

Gradient optimization in Euclidean space is straightforward, while for spherical or hyperbolic embeddings, we have to additionally control that points belong to a surface. In previous works, Riemann-SGD was used to solve this problem [2]. In short, it projects Euclidean gradients on the tangent space at a point and then uses a so-called exponential map to move the point along the surface according to the gradient projection. For product spaces, a generalization of the exponential map has been proposed [5, 26].

In [28], the authors compare RSGD with the retraction technique, where points are moved along the gradients in the ambient space and are projected onto the surface after each update. From their experiment, the retraction technique requires from 2% to 46% more iterations, depending on the learning rate. However, the exponential update step takes longer. Hence the advantage of RSGD in terms of computation time depends on the specific implementation.

### 3 Overlapping spaces

#### 3.1 Overlapping spaces

In this section, we propose a new concept of *overlapping spaces*. This concept generalizes product spaces and allows us to make the signature (types and dimensions of combined spaces) trainable. Our main idea is to divide the embedding vector into several *overlapping* (unlike product spaces) segments, each segment corresponding to its own space. Then, instead of discrete signature brute-forcing, we optimize the weights of the signature elements.

Importantly, we allow the same coordinates of an embedding vector to define distances in spaces of different geometry. For this purpose, we need to map a vector  $x \in \mathbb{R}^d$  (for any  $d \geq 1$ ) to a point in Euclidean, hyperbolic, and spherical space. Let us denote this mapping by  $M$ . Obviously, for Euclidean space, we may take  $M_E(x) = x$ . We may use the vector normalization for spheres, and for  $H_d$  we use a projection from a hyperplane to a hyperboloid:

$$M_S(x) = \frac{x}{|x|} \in S_{d-1}, M_H(x) = \left( \sqrt{1 + \sum_{i=2}^d x_i^2}, x_1, \dots, x_d \right) \in H_d. \quad (4)$$

Note that for such parametrization a  $d$ -dimensional vector  $x$  is mapped into Euclidean and hyperbolic spaces of dimension  $d$  and into a spherical space of dimension  $d - 1$ . Hence, in standard implementations of product spaces, a sphere  $S_d$  is parametrized by  $d + 1$ -dimensional vector [9]. However, this requires more coordinates to be stored for each spherical space. Hence, to make a fair comparison of all spaces, we use the hyperspherical coordinates for  $S_d$ :

$$\hat{M}_S(x) = \begin{pmatrix} \cos x_1 & \cos x_2 & \dots & \cos x_{d-1} & \cos x_d \\ \cos x_1 & \cos x_2 & \dots & \cos x_{d-1} & \sin x_d \\ \cos x_1 & \cos x_2 & \dots & \sin x_{d-1} & \\ \dots & & & & \\ \sin x_1 & & & & \end{pmatrix} \in S_d. \quad (5)$$

Now we are ready to define an overlapping space. Consider two vectors  $x, y \in \mathbb{R}^d$ . Let  $p_1, \dots, p_k$  denote some subsets of coordinates, i.e.,  $p_i \subset \{1, \dots, d\}$ . We assume that together these subsets cover all coordinates, i.e.,  $\cup_{i=1}^k p_i = \{1, \dots, d\}$ . By  $x[p_i]$  we denote a subvector of  $x$  induced by  $p_i$ . Let  $D_i \in \{E, S, H\}$ . We define  $d_i(x, y) = d_{D_i}(M_{D_i}(x[p_i]), M_{D_i}(y[p_i]))$  and aggregate these distances with arbitrary positive weights  $w_1 \dots w_k \in \mathbb{R}_+$ :

$$d_O^0(x, y) = \max(w_1 d_1(x, y), \dots, w_k d_k(x, y)), \quad (6)$$

$$d_O^1(x, y) = \sum_{i=1}^k w_i d_i(x, y), \quad d_O^2(x, y) = \left( \sum_{i=1}^k w_i d_i^2(x, y) \right)^{1/2}.$$

**Definition 1.**  $O_d = \{x \in \mathbb{R}^d\}$  equipped with a distance  $d_O^0$ ,  $d_O^1$ , or  $d_O^2$  defined in (6) is called an overlapping space. This space is defined by  $p_i$ ,  $D_i$ , and  $w_i$ .

Note that it is sufficient to assume that spherical and hyperbolic spaces have curvatures 1 and  $-1$ , respectively, since changing curvature is equivalent to changing scale, which is captured by  $w_i$ . The following statement follows from the definition above and from the fact that  $d_E$ ,  $d_S$ , and  $d_H$  are distances.

**Statement 1.** If  $\cup_{i=1}^k p_i = \{1, \dots, d\}$  and  $w_1 \dots w_k \in \mathbb{R}_+$ , then  $d_O^0$ ,  $d_O^1$ ,  $d_O^2$  are distances on  $\mathbb{R}^d \times \mathbb{R}^d$ , i.e., they satisfy the metric axioms.

It is easy to see that overlapping spaces generalize product spaces. Indeed, if we assume  $p_i \cap p_j = \emptyset$  for all  $i \neq j$ , then an overlapping space reduces to a product space. However, the fact that we allow  $p_i \cap p_j \neq \emptyset$  gives us a significantly larger expressive power for the same dimension  $d$ .

### 3.2 Generalization with WIPS: OS-Mixed measure

Surprisingly, in our experiments, we notice that in some cases, the non-metric methods can successfully be used for graph embeddings even with the distortion loss, where model approximates metric distances. A shortcoming of such measures is that they cannot be converted to a distance via a monotone transformation. On the other hand, for ranking loss functions, weighted and standard dot products can have good performance [13].

To close the gap between metric and non-metric methods, we propose a generalization of the overlapping spaces that also includes weighted inner product similarity (WIPS): we extend the list of base distance functions  $\{d_E, d_S, d_H\}$  with  $d_{\text{dot}} = c - x^T y$ . Note that by mixing such ‘distance’ function with all possible subsets  $p_i \in 2^{\{1 \dots d\}}$  using  $l1$ -aggregation (6), we get WIPS measure

$$d_W = \tilde{c} - \sum_{i=1}^d \tilde{w}_i x_i y_i, \text{ where } \tilde{c} \text{ and } \tilde{w}_i \text{ are trainable values.}$$

Next, we suggest using an extended set of base distances  $\{d_E, d_S, d_H, d_W\}$  together, as shown in equation (6). It will be shown that this design gives very good results for both distortion and ranking versions of the graph reconstruction task. We further refer to this approach as *OS-Mixed*.

## 4 Optimization in overlapping spaces

### 4.1 Universal signature

Overlapping spaces defined in Sections 3 and 3.2 are flexible and allow capturing various geometries. However, similarly to product spaces, they need a signature ( $p_i$  and  $D_i$ ) to be chosen in advance. This section shows that a universal signature can be chosen, so no brute-force is needed to choose the best signature for a particular dataset.

Let  $t \geq 0$  denote the depth (complexity) of the signature for a  $d$ -dimensional embedding. Each layer  $l$ ,  $0 \leq l \leq t$ , of the signature consists of  $2^l$  subsets of coordinates:  $p_i^l = \{[d(i-1)/2^l] + 1, \dots, [di/2^l]\}$ ,  $1 \leq i \leq 2^l$ . Each  $p_i^l$  is associated with Euclidean, spherical, and hyperbolic spaces simultaneously. The corresponding weights are denoted by  $w_i^{l,E}, w_i^{l,S}, w_i^{l,H}$ . Then, the distance is computed according to (6). See Figure 1 for an illustration of the procedure (for  $d = 10$  and  $t = 1$ ).

Informally, we first consider the original vectors  $x, y$  and compute Euclidean, spherical, and hyperbolic distances between them. Then, we split the vectors into two halves, and for each half, we also compute all three distances, and so on. Finally, all the obtained distances are averaged with the weights coefficient according to (6). Note that we have  $3(2^{t+1} - 1)$  different weights in our structure in general, but with  $l2$ -aggregation this value may be reduced to  $2(2^{t+1} - 1) + 2^t$  since for the Euclidean space, the distances between subvectors at the upper layers can be split into terms corresponding to smaller subvectors, so we essentially need only the last layer with  $2^t$  terms.

Recall that in product spaces, the weights correspond to curvatures of the combined spaces. In our case, they also play another important role: weights allow us to balance between different spaces. Indeed, for each subset of coordinates, we simultaneously compute the distance between the points assuming each of the combined spaces. Varying the weights, we can increase or decrease the contribution of a particular space to the distance. As a result, our signature allows us to learn the optimal signature, which does not have to be a product space since all weights can be non-zero. Note that the procedure described in this section naturally extends to OS-Mixed by adding the corresponding ‘distance’ to Euclidean, hyperbolic, and spherical.

### 4.2 Optimization

In this section, we describe how we embed into the overlapping space. Although Riemann-SGD (see Section 2.3) is a good solution from the theoretical point of view, in practice, due to errors in storing and processing real numbers, it may cause some problems. A point that we assume to lie on a surface (sphere or hyperboloid) does not numerically lie on it usually. Due to the accumulation of numerical errors, with each iteration of RSGD, the point may move away from the surface. Therefore, in practice, after each step, all embeddings are explicitly projected onto the surface, which may slow down the algorithm. Moreover, RSGD is not applicable if one needs to process the output of a neural network,

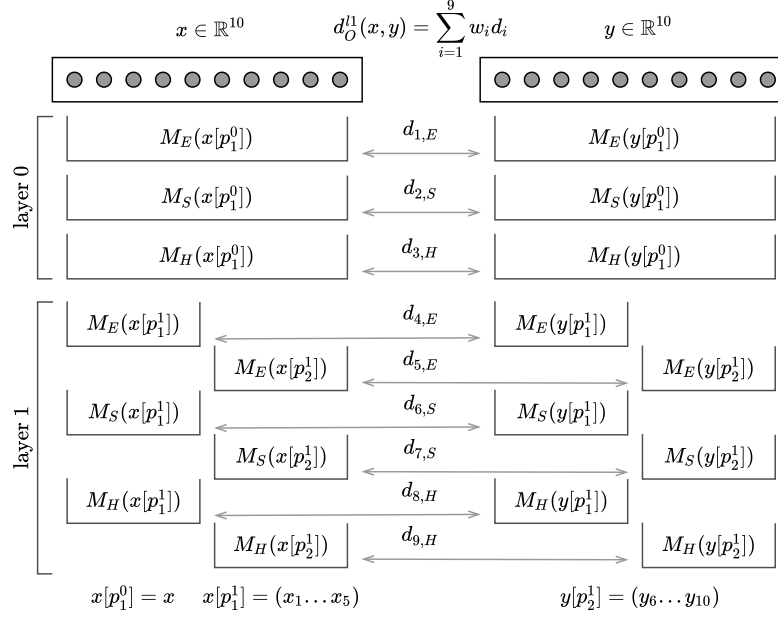


Figure 1: Overlapping space with  $d = 10$ ,  $t = 1$ , and  $l1$  (sum) aggregation

which cannot be required to belong to a given surface (e.g., to satisfy  $\langle x, x \rangle_h = 1 \Leftrightarrow x \in H_d$ ). As a result, before finding the hyperbolic distance between two outputs of a neural network in Siamese [3] setup, one first needs to somehow map them to a hyperboloid.

Instead of RSGD, we store the embedding vectors in Euclidean space and calculate distances between them using the mappings (4) to the corresponding surfaces. Thus, we can evaluate the distances between the outputs of neural networks and also use conventional optimizers. To optimize embeddings, we first map Euclidean vectors into the corresponding spaces, calculate distances and loss function, and then backpropagate through projection functions. To improve the convergence, we use Adam [14] instead of the standard SGD. Applying this to product spaces, we achieve the results similar to the original paper [9] (see Table 2 of the supplemental material), where RSGD was used with the learning rate brute-forcing, custom learning rate for curvature coefficients, and other tricks.

## 5 Experiments

### 5.1 Compared spaces

In this section, we provide a thorough analysis to compare all metric spaces discussed in the paper, including product spaces with all signatures from [9] and the proposed overlapping space. For the non-metric distance (similarity) functions, we consider  $d(x, y) = c - x^T y$ ,  $d(x, y) = c - \sum w_i x_i y_i$  (WIPS),  $d(x, y) = c \exp(-x^T y)$  with trainable parameters  $c, w_i \in \mathbb{R}$ , and the proposed OS-Mixed measure. We add them to analyze whether they are able to approximate graph distances in distortion setup. Similarly to [9], we fix the dimension  $d = 10$ . However, for a fair comparison, we fix the number of *stored values* for each embedding and used hyperspherical parametrization (5) instead of just storing  $d + 1$  coordinates.<sup>4</sup> The training details are given in Supplemental A. The code of our experiments supplements the submission.

### 5.2 Graph reconstruction

**Graph datasets** We use the following graph datasets: the USCA312 dataset of distances between North American cities [4] (weighted complete graph), a graph of computer science Ph.D. advisor-

<sup>4</sup>In Supplemental B.2, we evaluate spherical spaces without this modification to compare with [9].

Table 1: Datasets for graph reconstruction

	UCSA312	CS PhDs	Power	Facebook	WLA6	EuCore
Nodes	312	1025	4941	4039	3227	986
Edges	48516 (weighted)	1043	6594	88234	3604	16687

Table 2: Distortion graph reconstruction, top results are highlighted, top metric results are underlined

Signature	UCSA312	CS PhDs	Power	Facebook	WLA6	EuCore
$E_{10}$	<b><u>0.00318</u></b>	0.0475	0.0408	0.0487	0.0530	0.1242
$H_{10}$	0.01104	0.0443	0.0348	0.0483	<u>0.0279</u>	0.1144
$S_{10}$	0.01065	0.0519	0.0453	0.0561	0.0608	0.1260
$H_5^2 \equiv H_5 \times H_5$	0.00573	0.0345	0.0255	0.0372	<u>0.0279</u>	<u>0.1106</u>
$S_5 \times S_5 \equiv S_5^2$	0.00700	0.0501	0.0438	0.0552	<u>0.0584</u>	0.1251
$H_5 \times S_5$	0.00541	<u>0.0341</u>	<u>0.0254</u>	<u>0.0346</u>	0.0310	0.1195
$H_2^5$	0.00592	0.0344	0.0273	0.0439	0.0356	0.1163
$S_2^5$	0.00604	0.0464	0.0416	0.0512	0.0543	0.1244
$H_2^2 \times E_2 \times S_2^2$	0.00537	0.0344	0.0302	0.0406	0.0437	0.1193
$O_{l1}, t = 0$	<b><u>0.00324</u></b>	0.0368	0.0281	0.0458	0.0286	0.1141
$O_{l1}, t = 1$	<u>0.00325</u>	<b><u>0.0300</u></b>	<b><u>0.0231</u></b>	<u>0.0371</u>	<u>0.0272</u>	<u>0.1117</u>
$O_{l2}, t = 1$	0.00530	<u>0.0328</u>	<b><u>0.0246</u></b>	<u>0.0324</u>	<u>0.0278</u>	<u>0.1127</u>
$c - \text{dot}$	0.04005	0.0412	0.0461	0.0236	0.0296	0.1085
$c - \text{wips}$	0.06468	0.0358	0.0442	<b><u>0.0161</u></b>	<b><u>0.0238</u></b>	<b><u>0.1016</u></b>
$ce^{-\text{dot}}$	0.08142	0.0424	0.0505	0.0192	0.0270	0.1048
$O_{mix-l1}, t = 1$	<b><u>0.00277</u></b>	<b><u>0.0243</u></b>	<b><u>0.0235</u></b>	<b><u>0.0172</u></b>	<b><u>0.0187</u></b>	<b><u>0.1026</u></b>
$O_{mix-l2}, t = 1$	0.00464	<b><u>0.0220</u></b>	0.0258	<b><u>0.0163</u></b>	<b><u>0.0198</u></b>	<b><u>0.1028</u></b>

advisee relationships [1], a power grid distribution network with backbone structure [27], a dense social network from Facebook [16], and EuCore dataset generated using email data from a large European research institution [15]. We also created a new dataset, obtained by launching the breadth-first search on the Wikipedia category graph, starting from the “Linear Algebra” category with search depth limited to 6. Further, we refer to this dataset as WLA6; more details are given in Supplemental A.2. This graph is very close to being a tree, although it has some cycles. We expect the hyperbolic space to give a significant profit for this graph, and we observe that product spaces give almost no additional advantage. The purpose of using this additional dataset is to evaluate overlapping spaces on a dataset where product spaces do not provide quality gains. Table 1 lists the properties of all considered datasets.

**Distortion loss** We start with the standard graph reconstruction task with distortion loss (1). The goal is to embed all nodes of a given graph into a  $d$ -dimensional space approximating the pairwise graph distances between the nodes. In this setup, all models are trained to minimize distortion (1), the results are shown in Table 9. It can be seen that the overlapping spaces outperform other metric spaces, and the best overlapping space (among considered) is the one with  $l1$  aggregation and complexity  $t = 1$ . Interestingly, the performance of such overlapping space is often better than for the *best* product space.

Simple non-metric distance functions show highly unstable results for this task: for the UCSA312 dataset, the obtained distortion is orders of magnitude worse than the best one. However, on some datasets (Facebook and WLA6), the performance is quite good, and for Facebook, these similarities have much better performance than all metric solutions. We conclude that such functions are worth trying for the graph reconstruction with the distortion loss, but their performance is unstable. In contrast, the overlapping spaces show good and stable results on all datasets, and the proposed OS-Mixed modification (see Section 3.2) outperforms all other approaches.

**Ranking loss** As discussed in Section 2.1, in many practical applications, only the order of the nearest neighbors matters. In this case, it is more reasonable to use mAP (2). In previous work [9], mAP was also reported, but the models were trained to minimize distortion. In our experiments, we observed that distortion optimization weakly correlates with mAP optimization. Hence, we minimize

Table 3: mAP graph reconstruction, top results are highlighted, top metric results are underlined

Signature	UCSA312	CS PhDs	Power	Facebook	WLA6	EuCore
$E_{10}$	0.9290	0.9487	0.9380	0.7876	0.7199	0.6108
$H_{10}$	0.9173	0.9399	0.9385	0.7997	0.9617	0.6670
$S_{10}$	0.9183	0.9519	0.9445	0.7768	0.7289	0.6037
$H_5^2$	0.9247	0.9481	0.9415	0.8084	<u>0.9682</u>	<u>0.6783</u>
$S_5^2$	0.9316	0.9600	0.9482	0.7790	0.7307	0.6116
$H_5 \times S_5$	0.9397	0.9538	0.9505	0.7947	<u>0.9751</u>	<u>0.6847</u>
$H_2^5$	0.9364	0.9671	0.9508	0.7979	0.8597	0.6611
$S_2^5$	0.9439	0.9656	0.9511	0.7800	0.7358	0.6169
$H_2^2 \times E_2 \times S_2^2$	0.9519	0.9638	0.9507	0.7873	0.7794	0.6492
$O_{l1}, t = 0$	<u>0.9538</u>	<u>0.9879</u>	<u>0.9728</u>	<u>0.8093</u>	0.6759	0.6580
$O_{l1}, t = 1$	<b>0.9522</b>	<b>0.9904</b>	<u>0.9762</u>	<u>0.8185</u>	0.9598	0.6691
$O_{l2}, t = 1$	<u>0.9522</u>	<u>0.9938</u>	<u>0.9907</u>	<u>0.8326</u>	<u>0.9694</u>	<u>0.7078</u>
$c - \text{dot}$	<b>1</b>	<b>1</b>	<b>0.9983</b>	<b>0.8745</b>	<b>0.9990</b>	0.7409
$c - \text{wips}$	<b>1</b>	<b>1</b>	<b>1</b>	0.8704	<b>1</b>	<b>0.7742</b>
$O_{mix-l1}, t = 1$	<b>1</b>	<b>1</b>	<b>0.9994</b>	<b>0.8806</b>	<b>0.9997</b>	<b>0.7860</b>
$O_{mix-l2}, t = 1$	<b>1</b>	<b>1</b>	<b>1</b>	<b>0.9021</b>	<b>1</b>	<b>0.8405</b>

Table 4: DSSM results, top three results are highlighted

Signature	Test mAP	Signature	Test mAP
$E_{10}$	0.4459	$E_{256}$	<b>0.717</b>
$H_{10}$	0.4047	$H_{256}$	0.412 <sup>5</sup>
$S_{10}$	0.4364	$S_{255}$	0.588
$H_5^2$	0.4492	$H_{128}^2$	0.547
$S_5^2$	<b>0.4573</b>	$S_{127}^2$	0.662
$H_5 \times S_5$	0.3295	$H_{128} \times S_{127}$	0.501
$H_2^5$	0.3681	$H_{61}^4 \times H_{62}$	0.621
$S_2^5$	<b>0.4616</b>	$S_{60}^4 \times S_{61}$	<b>0.701</b>
$H_2^2 \times E_2 \times S_2^2$	0.3526	$c - \text{dot}$	<b>0.738</b>
$c - \text{dot}$	0.4194	$O_{l1}, t = 0$	0.677
$O_{l1}, t = 0$	<b>0.4562</b>	$O_{l1}, t = 1$	0.662
$O_{l1}, t = 1$	0.4498	$O_{mix-l1}, t = 1$	0.663
$O_{l2}, t = 1$	0.4456	$O_{mix-l2}, t = 1$	0.655
$O_{mix-l1}, t = 1$	0.4447		
$O_{mix-l2}, t = 1$	0.4483		

the proxy-loss defined in equation (3). The results are shown in Table 10, and the obtained values for mAP are indeed much better than the ones obtained with distortion optimization [9], i.e., it is important to use an appropriate loss function. According to Table 10, among the metric spaces, the best results are achieved with the overlapping spaces (especially for  $l2$ -aggregation with  $t = 1$ ). However, in contrast to distortion loss, ranking based on the dot-product outperforms all metric spaces. However, using OS-Mixed measure allows us to improve these results further.

### 5.3 DSSM experiment

From a practical perspective, it is also important to analyze whether an embedding can generalize to unseen examples. For instance, an embedding can be made via a neural network based on objects' characteristics, such as text descriptions or images. This section analyzes whether it is reasonable to use complex geometries, including product spaces and overlapping spaces, in such a scenario.

For this purpose, we trained a classic DSSM model [11]<sup>6</sup> on a private Wikipedia search dataset consisting of 491044 pairs (search query, relevant page), examples are given in the supplemental material. All queries are divided into train, validation, and test sets, and for each signature, the

<sup>5</sup>The gap between  $E_{256}$  and  $H_{256}$  may seem suspicious, but in Table 5 of [9] a similar pattern is observed.

<sup>6</sup>We changed dense layers sizes in order to achieve the required embedding length and used more complex text tokenization with char bigrams, trigrams, and words, instead of just char trigrams.



Table 5: Bipartite graph reconstruction (short version)

	mAP	distortion
best metric space (type)	0.824 ( $O_{l1}, t = 0$ )	0.082 ( $O_{l1}, t = 1$ )
$c - \text{dot}$	<b>0.863</b>	<b>0.079</b>
$c - \text{wips}$	1	0.091
$O_{mix-l2}, t = 1$	1	0.070

Table 6: WIPS distortion (5 restarts; best learning rate)

	avg.	worst	best	std
$c - \text{wips}$	0.092	0.100	0.078	0.0078
$O_{mix-l2}, t = 1$	0.071	0.074	0.069	0.0018

optimal iteration was selected on the validation set. Table 4 compares all models for two embedding sizes. For short embeddings, we see that a product space based on spherical geometry is useful, and overlapping spaces have comparable quality. However, in large “industrial size” dimensions, the best results are achieved with the standard dot product, questioning the utility of complex geometries in the case of large dimensions.

Note that in DSSM-like models, the most time-consuming task is model training. Hence, training multiple models for choosing the best configuration can be infeasible. Hence, for small dimensions, overlapping spaces can be preferable over product spaces since they are universal and do not require parameter tuning. Moreover, calculating element embeddings is more time-consuming than calculating distances. Hence, even though calculating distances in the overlapping space has larger complexity than in simpler spaces, it does not have a noticeable effect in real applications.

#### 5.4 Synthetic bipartite graph reconstruction

Let us additionally illustrate that some graph structures are poorly embedded in the considered metric spaces. Our intuition is that the dot product is suitable for datasets in which a few objects are more popular than the other ones. Hence, we perform graph reconstruction on a synthetic bipartite graph with two sets of sizes 20 and 700 with 5% edge probability (isolated nodes were removed, and the remaining graph is connected). Clearly, there are a few popular nodes and many nodes of small degrees in the obtained graph. Table 5 compares the performance of the best metric space with the dot-product performance. As we can see, this experiment confirms our assumption that specific graphs are poorly embedded in metric spaces, even with distortion loss. We also see that our  $d_{O-Mixed}$  approach gives the best result with a margin. This additionally confirms the universality of the proposed approach. We also note that the optimization of WIPS is highly unstable on this dataset, see Table 6 for details.

## 6 Conclusion

This paper proposed the new concept of overlapping spaces that do not require signature brute-forcing and have better or comparable performance relative to the best product space in the graph reconstruction task. Improvements are observed for both global distortion and local mAP loss functions. In our experiments, we noticed that the conventional dot product often outperforms the best product space. An important advantage of our method is that it allows us to easily incorporate new distance or similarity as a building block. The obtained overlapping-mixed non-metric measure achieves the best results for both distortion and mAP. We also evaluated the proposed overlapping spaces in the DSSM setup, and in the case of short embeddings, product space gives a better result than standard spaces, and the OS is comparable to it. In the case of long embeddings, no profit from complex spaces was found.

## References

- [1] Phillip Bonacich. 2008. Book Review: W. de Nooy, A. Mrvar, and V. Batagelj Exploratory Social Network Analysis With Pajek. (2004). *Sociological Methods & Research - SOCIOL METHOD RES* 36 (05 2008), 563–564. <https://doi.org/10.1177/0049124107306674>
- [2] Silvere Bonnabel. 2013. Stochastic Gradient Descent on Riemannian Manifolds. *IEEE Trans. Automat. Control* 58 (2013), 2217–2229.
- [3] Jane Bromley, Isabelle Guyon, Yann LeCun, Eduard Säckinger, and Roopak Shah. 1994. Signature verification using a " siamese" time delay neural network. In *Advances in neural information processing systems*. 737–744.
- [4] John Burkardt. 2011. Cities – City Distance Datasets. <https://people.sc.fsu.edu/~jburkardt/datasets/cities/cities.html>
- [5] Frederick Arthur Ficken. 1939. The Riemannian and affine differential geometry of product-spaces. (1939), 892–913.
- [6] Palash Goyal and Emilio Ferrara. 2018. Graph embedding techniques, applications, and performance: A survey. *Knowledge-Based Systems* 151 (2018), 78–94. <https://doi.org/10.1016/j.knosys.2018.03.022>
- [7] Mihajlo Grbovic, Vladan Radosavljevic, Nemanja Djuric, Narayan Bhamidipati, Jaikit Savla, Varun Bhagwan, and Doug Sharp. 2015. E-commerce in your inbox: Product recommendations at scale. In *Proceedings of the 21th ACM SIGKDD international conference on knowledge discovery and data mining*. 1809–1818.
- [8] Aditya Grover and Jure Leskovec. 2016. node2vec: Scalable Feature Learning for Networks. *CoRR* abs/1607.00653 (2016). arXiv:1607.00653 <http://arxiv.org/abs/1607.00653>
- [9] Albert Gu, Frederic Sala, Beliz Gunel, and Christopher Ré. 2019. Learning mixed-curvature representations in product spaces. *International Conference on Learning Representations (ICLR)* (2019).
- [10] Yifan Hu, Yehuda Koren, and Chris Volinsky. 2008. Collaborative Filtering for Implicit Feedback Datasets. In *IEEE International Conference on Data Mining (ICDM 2008)*. 263–272. <http://yifanhu.net/PUB/cf.pdf>
- [11] Po-Sen Huang, Xiaodong He, Jianfeng Gao, Li Deng, Alex Acero, and Larry Heck. 2013. Learning Deep Structured Semantic Models for Web Search using Clickthrough Data. *ACM International Conference on Information and Knowledge Management (CIKM)*.
- [12] Valentin Khruikov, Leyla Mirvakhabova, Evgeniya Ustinova, Ivan Oseledets, and Victor Lempitsky. 2020. Hyperbolic image embeddings. In *Proceedings of the IEEE/CVF Conference on Computer Vision and Pattern Recognition*. 6418–6428.
- [13] Geewook Kim, Akifumi Okuno, Kazuki Fukui, and Hidetoshi Shimodaira. 2019. Representation learning with weighted inner product for universal approximation of general similarities. *arXiv preprint arXiv:1902.10409* (2019).
- [14] Diederik Kingma and Jimmy Ba. 2014. Adam: A Method for Stochastic Optimization. *International Conference on Learning Representations* (12 2014).
- [15] Jure Leskovec, Jon Kleinberg, and Christos Faloutsos. 2007. Graph evolution: Densification and shrinking diameters. *ACM transactions on Knowledge Discovery from Data (TKDD)* 1, 1 (2007), 2–es.
- [16] Jure Leskovec and Julian J. McAuley. 2012. Learning to Discover Social Circles in Ego Networks. In *Advances in Neural Information Processing Systems* 25, F. Pereira, C. J. C. Burges, L. Bottou, and K. Q. Weinberger (Eds.). Curran Associates, Inc., 539–547. <http://papers.nips.cc/paper/4532-learning-to-discover-social-circles-in-ego-networks.pdf>

- [17] Weiyang Liu, Yandong Wen, Zhiding Yu, Ming Li, Bhiksha Raj, and Le Song. 2017. Sphereface: Deep hypersphere embedding for face recognition. In *Proceedings of the IEEE conference on computer vision and pattern recognition*. 212–220.
- [18] Tomas Mikolov, Kai Chen, Greg Corrado, and Jeffrey Dean. 2013. Efficient Estimation of Word Representations in Vector Space. *CoRR* abs/1301.3781 (2013). <http://dblp.uni-trier.de/db/journals/corr/corr1301.html#abs-1301-3781>
- [19] Maximillian Nickel and Douwe Kiela. 2017. Poincaré embeddings for learning hierarchical representations. In *Advances in neural information processing systems*. 6338–6347. <http://papers.nips.cc/paper/7213-poincare-embeddings-for-learning-hierarchical-representations.pdf>
- [20] Maximillian Nickel and Douwe Kiela. 2018. Learning Continuous Hierarchies in the Lorentz Model of Hyperbolic Geometry. In *International Conference on Machine Learning*. 3776–3785. <https://arxiv.org/abs/1806.03417>
- [21] Jeffrey Pennington, Richard Socher, and Christopher D. Manning. 2014. GloVe: Global Vectors for Word Representation. In *Empirical Methods in Natural Language Processing (EMNLP)*. 1532–1543. <http://www.aclweb.org/anthology/D14-1162>
- [22] Bryan Perozzi, Rami Al-Rfou, and Steven Skiena. 2014. DeepWalk: Online Learning of Social Representations. *CoRR* abs/1403.6652 (2014). arXiv:1403.6652 <http://arxiv.org/abs/1403.6652>
- [23] Gang Qian, Shamik Sural, Yuelong Gu, and Sakti Pramanik. 2004. Similarity between Euclidean and Cosine Angle Distance for Nearest Neighbor Queries. In *Proceedings of the 2004 ACM Symposium on Applied Computing (SAC '04)*. Association for Computing Machinery, New York, NY, USA, 1232–1237. <https://doi.org/10.1145/967900.968151>
- [24] Frederic Sala, Chris De Sa, Albert Gu, and Christopher Re. 2018. Representation Tradeoffs for Hyperbolic Embeddings. In *International Conference on Machine Learning*. 4457–4466.
- [25] Alexandru Tifrea, Gary Bécigneul, and Octavian-Eugen Ganea. 2018. Poincaré GloVe: Hyperbolic Word Embeddings. *arXiv preprint arXiv:1810.06546* (2018).
- [26] Pavan K Turaga and Anuj Srivastava. 2016. *Riemannian Computing in Computer Vision*. Springer.
- [27] Steven H Watts, Duncan J. Strogatz. 1998. *Collective Dynamics of Small-World Networks*. *Nature*. 393:440 – 442. [https://doi.org/10.1007/978-3-658-21742-6\\_130](https://doi.org/10.1007/978-3-658-21742-6_130)
- [28] Benjamin Wilson and Matthias Leimeister. 2018. Gradient descent in hyperbolic space. *arXiv preprint arXiv:1805.08207* (2018).
- [29] Richard C Wilson, Edwin R Hancock, Elżbieta Pekalska, and Robert PW Duin. 2014. Spherical and hyperbolic embeddings of data. *IEEE transactions on pattern analysis and machine intelligence* 36, 11 (2014), 2255–2269.

## A Experimental Setup

### A.1 Training Details

All models discussed in Section 5.2 were trained with 2000 iterations. If more than one learning rate was used for a certain dataset (due to problems with the convergence of individual models), all the spaces were evaluated for all learning rates, and the best result was reported for each space. For distortion, the learning rate was 0.1 for all datasets except UCSA312 (Cities), where we had 0.1 and 0.01. For mAP, the learning rate 0.1 was used for all datasets except UCSA312 and CSpHds, where we had 0.01 and 0.05 for both datasets.

For the experiments in Section 5.3, we used 5000 iterations for short embeddings and 1000 for long ones (long embeddings converged faster). Hard-negative mining was not used for DSSM training. Instead, large batches of 4096 random training examples (almost 1% of the entire dataset) were used. During the learning process, only the training queries and documents were used. For evaluation, the nearest website was searched among all the documents. The training part was 90% of the dataset, and the quality discrepancy between validation and test sets was quite small. Data samples are given in the table 12.

For the synthetic experiment in Section 5.4, for all spaces, the learning rates 0.1, 0.05, 0.01, 0.001 were used, and the best result was selected. We had 2000 and 1000 iterations for distortion and mAP, respectively.

### A.2 WLA6 Dataset Details

As described in the main text, this dataset is obtained by running the breadth-first search algorithm on the category graph of the English-language Wikipedia (<https://en.wikipedia.org/wiki/Special:CategoryTree>), starting from the vertex (category) “Linear algebra” and limited to the depth 6 (Wikipedia Linear Algebra 6). We provide this graph along with the texts (names) of the vertices (categories). The resulting graph is very close to being a tree, although there are some cycles. Predictably, hyperbolic space gives a significant profit for this graph, while using product spaces gives almost no additional advantage. The purpose of using this dataset is to check our conclusions on data other than those used in [9] and to evaluate overlapping spaces on a dataset where product spaces do not provide quality gains. Figure 2 visualizes the obtained graph. Table 7 shows full version of the results.

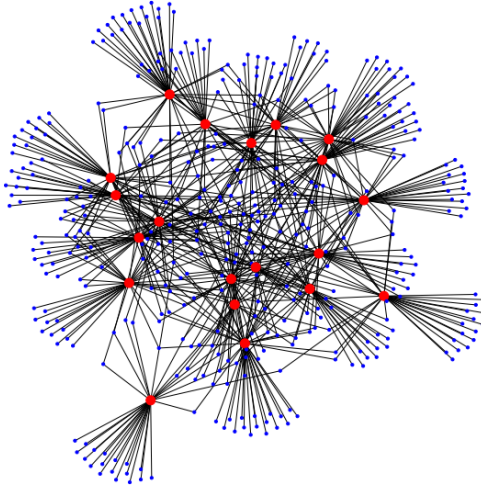


Figure 2: Graph visualization. Red (big) nodes belong to the smaller part.

Table 7: Bipartite graph reconstruction (full version)

	mAP	distortion
$E_{10}$	0.777	0.094
$H_{10}$	0.794	0.095
$S_{10}$	0.796	0.096
$H_5^2$	0.799	0.090
$S_5^2$	0.796	0.094
$H_5 \times S_5$	0.798	0.090
$H_2^5$	0.761	0.086
$S_2^5$	0.773	0.092
$H_2^2 \times E_2 \times S_2^2$	0.796	0.089
$O_{l1}, t = 0$	0.824	0.094
$O_{l1}, t = 1$	0.803	0.082
$O_{l2}, t = 1$	0.814	0.092
best metric space	0.824	0.082
$c - \text{dot}$	<b>0.863</b>	<b>0.079</b>
$c - \text{wips}$	1	0.091
$O_{mix-l1}, t = 1$	0.986	0.083
$O_{mix-l2}, t = 1$	1	0.070

## B Additional Experimental Results

### B.1 Our Implementation of Product Spaces vs Original One

Table 8 compares our implementation with the results reported in [9]. It should be noted that we have significantly different algorithms with differing numbers of iterations.

The optimal values of distortion obtained with our algorithm (except for the UCSA312 dataset) are comparable and usually better than those reported in [9]. On UCSA312, the obtained distortion is orders of magnitude better, which can be caused by the proper choice of the learning rate (in our experiments on this dataset, this choice significantly affected the results). These results indicate that our solution is a good starting point to compare different spaces and similarities.

For mAP, we optimize the proxy-loss, in contrast to the canonical implementation, where both metrics were specified for models trained with distortion. Clearly, the results are more stable for our approach: we do not have such a large spread of values for different spaces. We noticed that directly optimizing ranking losses leads to significant improvements.

### B.2 Parametrization of Spherical Space

In Tables 2 and 3 of the main text, we used hyperspherical parameterization of spherical subspaces in product spaces since we fixed the number of stored values for each space. Here, in Tables 9 and 10, we present the extended results, where we fix the mathematical dimension of product spaces and use  $d + 1$  parameters and simple mappings from Section 3.1, equation 4, as done in [9]. We can see that our implementation gives results comparable to the original ones in distortion setup and significantly better for mAP, which is associated with using the proxy-loss instead of distortion.

Table 8: Graph reconstruction: original product spaces vs our implementation

	UCSA312		CS PhDs		Power		Facebook	
	Canon.	Our	Canon.	Our	Canon.	Our	Canon.	Our
Distortion								
$E_{10}$	0.0735	0.0032	0.0543	0.0475	0.0917	0.0408	0.0653	0.0487
$H_{10}$	0.0932	0.0111	0.0502	0.0443	0.0388	0.0348	0.0596	0.0483
$S_{10}$	0.0598	0.0095	0.0569	0.0503	0.0500	0.0450	0.0661	0.0540
$H_5 \times H_5$	0.0756	0.0057	0.0382	0.0345	0.0365	0.0255	0.0430	0.0372
$S_5 \times S_5$	0.0593	0.0079	0.0579	0.0492	0.0471	0.0433	0.0658	0.0511
$H_5 \times S_5$	0.0622	0.0068	0.0509	0.0337	0.0323	0.0249	0.0402	0.0318
$H_2^5$	0.0687	0.0059	0.0357	0.0344	0.0396	0.0273	0.0525	0.0439
$S_2^5$	0.0638	0.0072	0.0570	0.0460	0.0483	0.0418	0.0631	0.0489
$H_2^2 \times E_2 \times S_2^2$	0.0765	0.0044	0.0391	0.0345	0.0380	0.0299	0.0474	0.0406
mAP								
$E_{10}$		0.9290	0.8691	0.9487	0.8860	0.9380	0.5801	0.7876
$H_{10}$		0.9173	0.9310	0.9399	0.8442	0.9385	0.7824	0.7997
$S_{10}$		0.9254	0.8329	0.9578	0.7952	0.9436	0.5562	0.7868
$H_5 \times H_5$		0.9247	0.9628	0.9481	0.8605	0.9415	0.7742	0.8084
$S_5 \times S_5$		0.9231	0.7940	0.9662	0.8059	0.9466	0.5728	0.7891
$H_5 \times S_5$		0.9316	0.9141	0.9654	0.8850	0.9467	0.7414	0.8087
$H_2^5$		0.9364	0.9694	0.9671	0.8739	0.9508	0.7519	0.7979
$S_2^5$		0.9281	0.8334	0.9714	0.8818	0.9521	0.5808	0.7915
$H_2^2 \times E_2 \times S_2^2$		0.9391	0.8672	0.9611	0.8152	0.9486	0.5951	0.7970

Table 9: Graph reconstruction with distortion loss, top results are highlighted, metrics only.

Signature	UCSA312	CS PhDs	Power	Facebook	WLA6
$E_{10}$	<b>0.00318</b>	0.0475	0.0408	0.0487	0.0530
$H_{10}$	0.01114	0.0443	0.0348	0.0483	<b>0.0279</b>
$S_{10}$	0.00951	0.0503	0.0450	0.0540	0.0589
$H_5^2 \equiv H_5 \times H_5$	0.00573	0.0345	0.0255	0.0372	<b>0.0279</b>
$S_5 \times S_5 \equiv S_5^2$	0.00792	0.0492	0.0433	0.0511	0.0585
$H_5 \times S_5$	0.00681	<b>0.0337</b>	<b>0.0249</b>	<b>0.0318</b>	0.0296
$H_2^5$	0.00592	0.0344	0.0273	0.0439	0.0356
$S_2^5$	0.00720	0.0460	0.0418	0.0489	0.0549
$H_2^2 \times E_2 \times S_2^2$	0.00436	0.0345	0.0299	0.0406	0.0405
$O_{l1}, t = 0$	<b>0.00356</b>	0.0368	0.0281	0.0458	0.0286
$O_{l1}, t = 1$	<b>0.00330</b>	<b>0.0300</b>	<b>0.0231</b>	<b>0.0371</b>	<b>0.0272</b>
$O_{l2}, t = 1$	0.00530	<b>0.0328</b>	<b>0.0246</b>	<b>0.0324</b>	<b>0.0278</b>

Table 10: Graph reconstruction with mAP ranking loss, top results are highlighted, metrics only.

Signature	UCSA312	CS PhDs	Power	Facebook	WLA6
$E_{10}$	0.9290	0.9487	0.9380	0.7876	0.7199
$H_{10}$	0.9173	0.9399	0.9385	0.7997	0.9617
$S_{10}$	0.9254	0.9578	0.9436	0.7868	0.7287
$H_5^2$	0.9247	0.9481	0.9415	0.8084	<b>0.9682</b>
$S_5^2$	0.9231	0.9662	0.9466	0.7891	0.7353
$H_5 \times S_5$	0.9316	0.9654	0.9467	0.8087	<b>0.9779</b>
$H_2^5$	0.9364	0.9671	0.9508	0.7979	0.8597
$S_2^5$	0.9281	0.9714	0.9521	0.7915	0.7346
$H_2^2 \times E_2 \times S_2^2$	0.9391	0.9611	0.9486	0.7970	0.6796
$O_{l1}, t = 0$	<b>0.9522</b>	<b>0.9879</b>	<b>0.9728</b>	<b>0.8093</b>	0.6759
$O_{l1}, t = 1$	<b>0.9522</b>	<b>0.9904</b>	<b>0.9762</b>	<b>0.8185</b>	0.9598
$O_{l2}, t = 1$	<b>0.9522</b>	<b>0.9938</b>	<b>0.9907</b>	<b>0.8326</b>	<b>0.9694</b>

Table 11: Comparison of proxy-losses, mAP

$P \sim$	UCSA312			CS PhD		
	$e^{-d}$	$e^{1/d}$	$1/d$	$e^{-d}$	$e^{1/d}$	$1/d$
$E_{10}$	0.929	0.911	0.899	0.949	0.956	0.831
$H_{10}$	0.917	0.807	0.885	0.940	0.749	0.764
$S_{10}$	0.925	0.797	0.838	0.958	0.572	0.689
$H_5^2$	0.925	0.890	0.883	0.948	0.976	0.723
$S_5^2$	0.923	0.802	0.858	0.966	0.748	0.775
$H_5 \times S_5$	0.932	0.838	0.865	0.965	0.804	0.721
$H_2^5$	0.936	0.896	0.903	0.967	0.998	0.823
$S_2^5$	0.928	0.856	0.871	0.971	0.876	0.881
$H_2^2 \times E_2 \times S_2^2$	0.939	0.872	0.865	0.961	0.884	0.689
$O_{l1}, t = 0$	0.952	0.933	0.872	0.988	0.961	0.762
$O_{l1}, t = 1$	0.952	0.947	0.877	0.990	0.963	0.815
$O_{l2}, t = 1$	0.952	0.939	0.880	0.994	0.979	0.810
$c - \text{dot}$	1	1	0.777	1	0.999	0.917

### B.3 Other Ways of Converting Distances to Probabilities

For the proxy-loss, we additionally experimented with other ways of converting distances to probabilities. Let us write  $L_{\text{proxy}}$  in the general form:

$$L_{\text{proxy}} = - \sum_{(v,u) \in E} \log P((v,u) \in E) = - \sum_{(v,u) \in E} \log \frac{t(d_U(f(v), f(u)))}{\sum_{w \in V} t(d_U(f(v), f(w)))}, \quad (7)$$

where  $t(d)$  is a function that decreases with distance  $d$ . We compare the following alternatives for  $t(d)$ :

$$t_1(d) = \exp(-d), t_2(d) = \exp\left(\frac{1}{\min(d, d_0)}\right), t_3(d) = \frac{1}{\min(d, d_0)},$$

where  $d_0$  is a small constant.

Recall that  $t_1$  was used in the main text and it seems to be the most natural choice.<sup>7</sup> Table 11 compares the options and shows that the best results are indeed achieved with  $t_1$ .

Table 12: Search query examples

Query	Web site
Kris Wallace	en.wikipedia.org/wiki/Chris_Wallace
1980: Mitsubishi produces one million cars...	en.wikipedia.org/wiki/Mitsubishi_Motors
code napoleon	en.wikipedia.org/wiki/Napoleonic_Code

<sup>7</sup>Note that this is the softmax over the inverted distances.